Fast and Slow Activation of Voltage-dependent Ion Channels in Radish Vacuoles

Franco Gambale, Alberto M. Cantu', Armando Carpaneto, and Bernhard U. Keller*
Istituto di Cibernetica e Biofisica, Via Dodecaneso 33, I-16146 Genova, Italy; *Max-Planck-Institut für biophysikalische Chemie, Am Faßberg, 37077 Göttingen, Germany

ABSTRACT The molecular processes associated with voltage-dependent opening and closing (gating) of ion channels were investigated using a new preparation from plant cells, i.e., voltage and calcium-activated ion channels in radish root vacuoles. These channels display a main single channel conductance of ~90 pS and are characterized by long activation times lasting several hundreds of milliseconds. Here, we demonstrate that these channels have a second kinetically distinct activation mode which is characterized by even longer activation times. Different membrane potential protocols allowed to switch between the fast and the slow mode in a controlled and reversible manner. At transmembrane potentials of −100 mV, the ratio between the fast and slow activation time constant was around 1:5. Correspondingly, activation times lasting several seconds were observed in the slow mode. The molecular process controlling fast and slow activation may represent an effective modulator of voltage-dependent gating of ion channels in other plant and animal systems.

INTRODUCTION

Voltage-dependent opening and closing (gating) of ion channels is a well studied phenomenon in a variety of channels in animal and plant cells (e.g., Hille (1992), Schroeder et al. (1987), Keller et al. (1989), Hedrich and Schroeder (1989) and references therein). The molecular basis of the gating process has been associated with the movement of charged gating particles sensing the membrane electric field. However, little or nothing is known about the molecular processes associated with the opening of single ion channels. It has been particularly difficult to monitor channel openings in animal cells as they are characterized by fast time constants (τ_{act} ~1 ms) and often masked by simultaneous channel inactivation. We have circumvented these problems by studying the opening of calcium-activated cation-selective channels from radish root vacuoles, which activate with typical time constants of several hundreds of milliseconds and do not inactivate. We investigated their activation properties with the patch clamp technique by using both whole-vacuole and single channel recordings. These measurements identified a fast and slow activation process of voltage-dependent ion channels in radish vacuoles.

METHODS

Isolation of vacuoles

The surface of a freshly cut radish root was rinsed with buffer solution and excised vacuoles were directly transferred into the patch clamp recording chamber. In a typical experiment, vacuoles were allowed to settle on the bottom of plastic petri dishes for 3–5 min. Before patch clamp measurements, the bath solution was perfused with the above saline to remove tissue not firmly attached to the bottom of the chamber.

Electrophysiology, data storage, and analysis

Patch clamp experiments were performed with standard patch clamp equipment (Hamill et al., 1981) on radish root vacuoles. Measurements were either performed in the attached patch configuration or in whole cell mode, which was obtained after breaking into the vacuole by a short voltage pulse 1–3 ms in duration and ~1 V in amplitude. The convention for the transmembrane vacuolar voltage was $V_m = V_{vacuole} - V_{cytosol}$, which is identical to the convention suggested by Hedrich and Neher (1988). Unless otherwise indicated the ionic concentrations in the bath and in the pipette were identical, i.e., KCl (200 mM), $CaCl_2$ (1 mM), $MgCl_2$ (2 mM), 4-morpholineethanesulfonic acid (25 mM), pH 6.4. Data were recorded with a standard EPC-7 patch clamp amplifier (List, Germany), low-pass filtered at 1 kHz with a four-pole Bessel filter and stored either on computer hard disk by using the Instrutech analysis software (Instrutech, USA) or directly on videotape. The kinetics of activation were evaluated as the time interval between the current at 20 and 80% of the maximum amplitude. The decay time constants were obtained by the best fit of decaying current with a single exponential function.

The single channel conductances and the corresponding error bars (in Fig. 2 *B*) were derived from the mean values and the standard deviations of the Gaussian distributions which gave the best fit for the current histograms. Histograms corresponding to the baseline and to the open state(s) were identified and the channel amplitude was deduced from the difference(s) between the current peaks. Single channel data were also obtained by using a different algorithm where events representative of single channel openings were individually identified. Within the limits of standard errors, the

Received for publication 15 January 1993 and in final form 10 August 1993.

0006-3495/93/11/1837/07 $2.00

two procedures gave identical results (e.g., differences were < 6% for data shown in Fig. 2 *B*).

RESULTS

Activation of vacuolar channels and whole cell currents

Patch clamp experiments were performed on vacuoles isolated from radish roots with standard patch clamp equipment (Hamill et al., 1981). Fig. 1 displays the result of an experiment that was performed in the whole-vacuole recording configuration. To investigate the voltage and time dependence of whole-vacuole currents, vacuolar membranes were exposed to a series of repetitive voltage steps which usually lasted 4 s. In most experiments, vacuoles were initially held at a membrane potential of 0 mV and then stepped to different negative and positive voltages between −100 mV and +100 mV. For cytoplasmic calcium concentrations above 10^{-5} M, this protocol induced voltage activated currents with maximum amplitudes of several nanoamperes at a holding potential of −110 mV (Fig. 1 *A*). Depending on the membrane potential, currents activated with time constants ranging from 300 to 500 ms. For a more detailed analysis, the charge carried by each current pulse was determined by integrating the current amplitude over the stimulus duration. As clearly shown in *B*, no charge transport was observed for positive membrane potentials, which is in line with previous results on the voltage dependence of vacuolar channels observed in other membrane systems (Hedrich and Neher, 1987; Pantoja et al., 1992a, 1992b).

Single channel currents

To investigate the molecular basis of the macroscopic currents, we performed single channel experiments in the vacuole-attached patch clamp configuration (Fig. 2 *A*). Single channel recordings from one or several ion channels were routinely observed after formation of a gigaseal between the glass pipette and the membrane surface of the vacuole. For a given membrane potential, single channel currents were characterized by a dominant single channel amplitude corresponding to a single channel conductance of approximately ~90 pS. Occasionally, smaller single channel events were observed, but they were discarded in the present analysis since they apparently gave a small contribution to the total current of the vacuole. The main single channel openings showed a linear voltage dependence, as exemplified in Fig. 2 *B*, and were mostly restricted to negative membrane voltages (*inset* in Fig. 2 *B*). These features correlated closely with the activation profile of the macroscopic currents observed in whole vacuole recordings which are displayed in Fig. 1.

The rapid closing (deactivation), the voltage dependence and the ionic selectivity of whole-vacuolar currents were investigated by using the experimental protocol shown on top of Fig. 3 *A*. In this experiment, the membrane potential was held at 0 mV and then stepped to a hyperpolarizing potential of −100 mV, which induced a fast activation of vacuolar channels. Subsequently, the channels were rapidly closed by repolarizing pulses of increasing amplitudes (voltage steps of +20 mV). Current signals obtained after membrane repolarisation (commonly denoted as "tail currents") showed a progressively higher percentage of channel closures for positive voltage steps. The maximum amplitude of tail currents was a linear function of voltage, both in symmetric and asymmetric ionic solutions, which is demonstrated in *B* and *D*, respectively. The decay time constants of tail currents, τ, are plotted as a function of voltage in *C*. As it is evident from the semilogarithmic plot, the decay times were well approximated by a monoexponential function of voltage with an

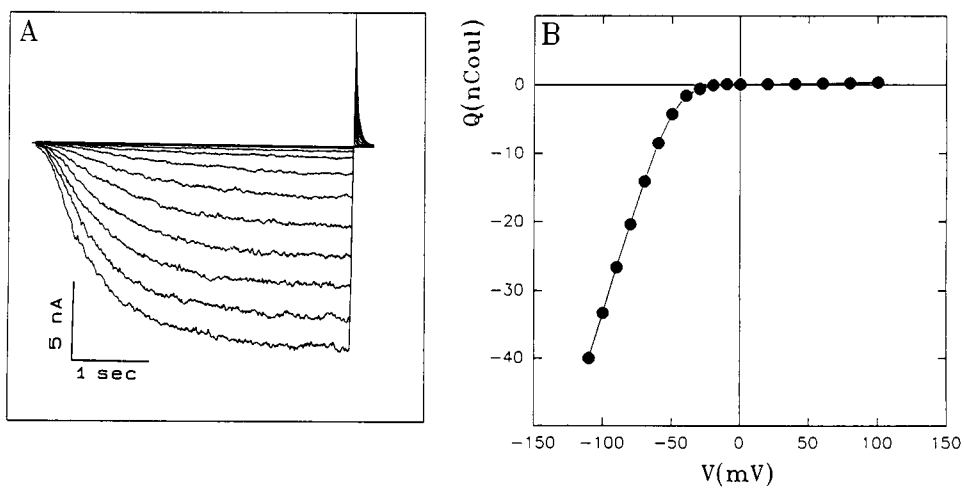

FIGURE 1 Macroscopic currents measured in whole-vacuole configuration. (*A*) Test pulses ranging between −110 and 100 mV, elicited inward currents at hyperpolarizing potentials, while almost no current was measured at positive voltages. Holding potential was 0 mV. Currents activated with time constants ranging between 300 and 500 ms. (*B*) Rectifying properties of vacuolar channels. The charge-voltage relationship is reported obtained by integrating the current over time during the stimulus. By convention, a negative sign indicates that the charge was obtained integrating negative inward current.

approximate time constant of 100 ms inferred for a voltage of 0 mV. This finding is in agreement with a kinetic scheme that contains only a single open state of the channel.

Whole-vacuole currents were strongly affected by the divalent cation concentration in the bath solution. For example, a decrease in the cytosolic calcium concentration from 1 to 0.1 mM completely suppressed the macroscopic current response as displayed in Fig. 4 *A*. Similarly, in the presence of 1 mM $CaCl_2$ the addition of 0.1 mM $ZnCl_2$ to the bath solution completely abolished the current response (Fig. 4 *B*). Taken together, these observations identify high cytosolic

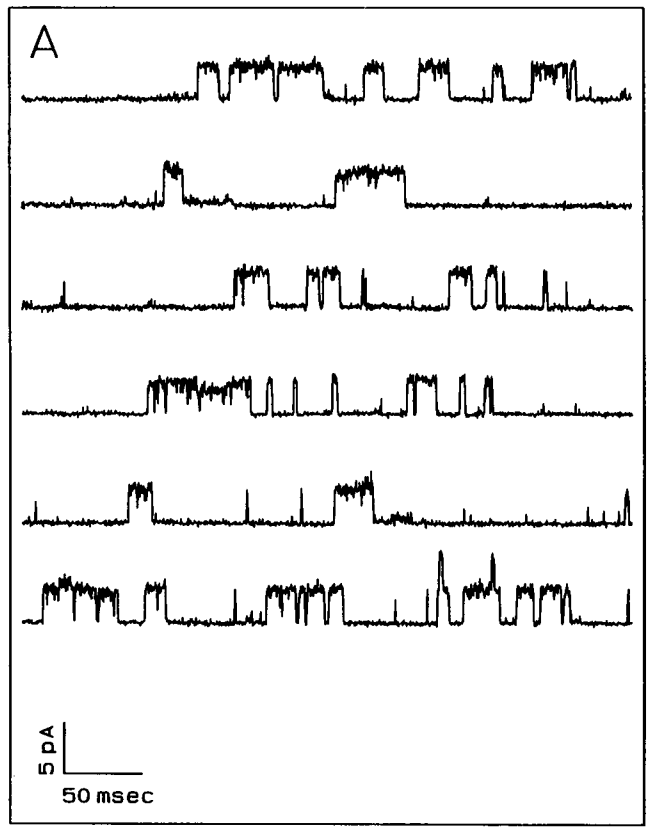

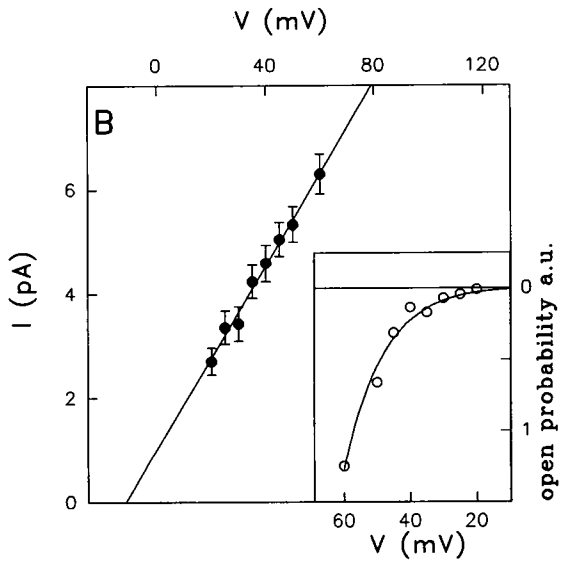

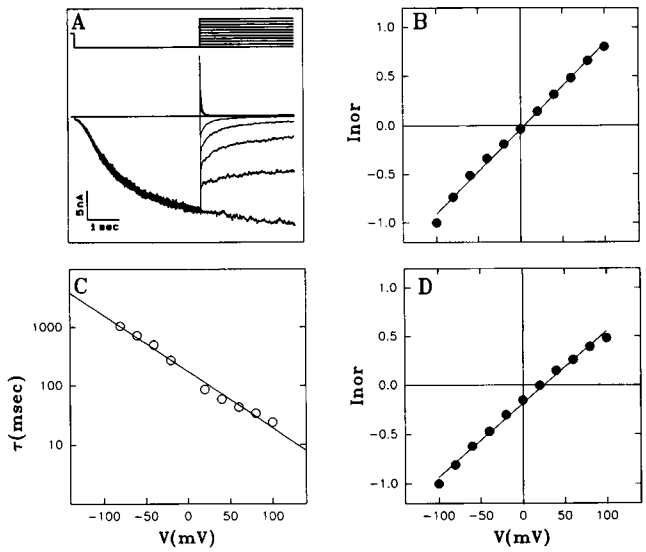

FIGURE 3 Selectivity and deactivation of vacuolar channels. (*A*) Tail currents were obtained stepping to different voltages ranging from −100 to +100 mV after the channel was opened by a step pulse to −100 mV. Symmetrical solutions (KCl (200 mM), $CaCl_2$ (1 mM), $MgCl_2$ (2 mM), pH 6.4). (*B*) The corresponding tail current peaks, I_{nor} (normalized with respect to the current measured at −100 mV), shows a linear dependence on the voltage of the stimulus. In *D* the same instantaneous IV plot was obtained in asymmetric conditions, in the presence of 217 mM KCl in the bath and 57 mM KCl in the pipette. The reversal potential at +28 mV indicated that the channel was selective for cations with a permeability ratio $P_{K^+}/P_{Cl^-} \sim 12$. (*C*) Time course for tail currents, τ, (represented in *B*) is plotted versus the voltage in semilogarithmic scale.

Ca^{2+} concentrations as an activator and Zn^{2+} as an effective blocker of channel activity. In both cases, for either 0.1 mM $CaCl_2$ or 1 mM $CaCl_2$/0.1 mM $ZnCl_2$, the current inhibition was complete and reversible. Moreover, the unimodal blocking actions suggested that the ion channels underlying the macroscopic vacuolar currents were homogeneous in their sensitivity for divalent cations. This underlines the notion that vacuolar currents are carried by a single population of channels which are indistinguishable in their response profile to different divalent cation concentrations.

Fast and slow activation of vacuolar channels

The long activation time of vacuolar channels allowed us to study in more detail the process of current activation and its

FIGURE 2 Single channel recordings from radish root vacuoles. (*A*) Typical single channels recorded in vacuole-attached configuration. It is immediate to see that all events present a dominant homogenous conductance of about 90 pS, even if a smaller channel with a conductance in the order of a few tens of picosiemens was occasionally observed in some experiments. Applied voltage was +35 mV. In *B* the single channel current voltage characteristics shows a linear behavior over the whole voltage range investigated. A single channel conductance of 88.4 ± 3.8 pS and a reversal potential of −11.4 ± 2.2 mV were inferred from this data. Each point was the result of at least 70 (at 20 mV) single events, for a total of 4654 events extracted from this experiment. Inset: from the same experiment the open time probability was plotted (in arbitrary units) as a function of the membrane voltage. For an easy comparison of these data (collected in the vacuole-attached configuration) with whole-vacuole current-voltage characteristics (Fig. 1 *B*), a mirror image of the *x-y* coordinate system was used.

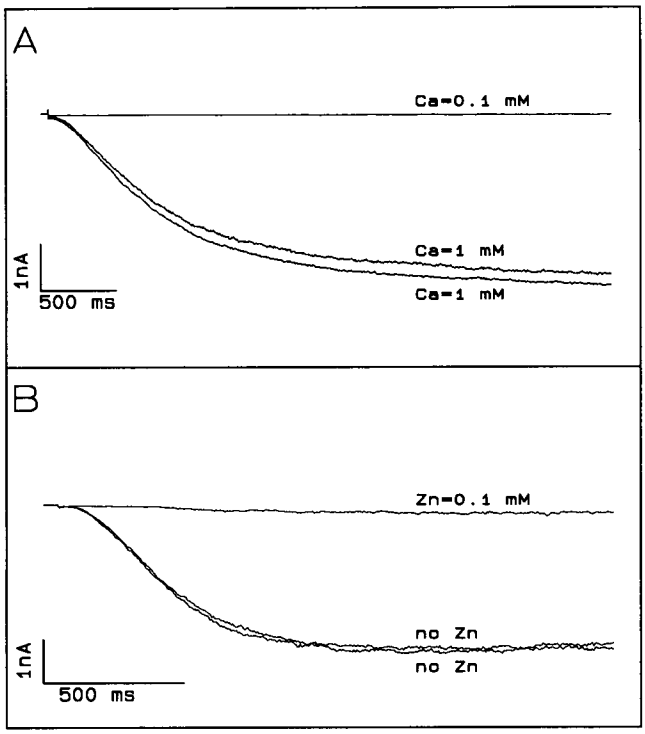

FIGURE 4 Calcium activates and zinc fully inhibited vacuolar currents. (*A*) When the cytoplasmic calcium concentration was decreased from 1 to 0.1 mM the whole-cell current of the radish vacuole completely vanished. The decrease of the current was completely reversible. (*B*) The addition of 0.1 mM $ZnCl_2$ to the cytoplasmic side reversibly and completely blocked the current. No residual current was observed in both cases. Ionic solutions in control and recovery were symmetric i.e. (in millimolar): KCl 200, $CaCl_2$ 1, $MgCl_2$ 2, pH 6.4. Currents were elicited by voltage steps to −100 mV from a holding potential of 0 mV.

modulation by different voltage protocols. Fig. 5 *A* displays a comparison of the current recordings obtained with two different protocols, e.g., stimulating the vacuole with intervals between voltage pulses ranging from 20 s (*curve 1*) to 300 ms (*curve 2*). At high frequency stimulation, currents were activated with a significantly slower time constant, around 1.8 s at V = −100 mV. As shown in the figure (*curve 3*), the change in activation time was completely reversible upon switching to the low frequency voltage protocol. Current amplitudes did not significantly change after switching between modes as it is clearly shown in Fig. 5 *B*. In this experiment longer stimuli were applied, which demonstrated that the steady state current levels had comparable amplitudes. These observations strongly suggest that in the steady state situation the same number of channels was activated by the two voltage protocols.

Fig. 6 displays current voltage relationships for the fast (*A*) and slow (*B*) activation mode obtained from the same vacuole. To keep channels in the fast mode, the interval between pulses was chosen to be 16 s for the currents displayed in Fig. 6 *A*. Current activation time constants were then measured as the time interval between the current at 20 and 80% of the maximum amplitude. In the fast mode, currents displayed activation time constants ranging from 300–500 ms. To transform channels to the slow activation mode, voltage pulses were repeated at higher frequency with a time interval shorter than 1 s (740 ms in Fig. 6 *B*). In this case, a clear change in the current voltage relation was observed. Most important, the activation time constant was clearly prolonged for all membrane voltages. The most significant observation was a fourfold prolongation of the activation time at −100 mV (see Fig. 6 *C*). Moreover, the switch between the two modes could be repeated several times in a controlled and reproducible way without an overall change in the basic current properties. This was demonstrated in experiments where the two modes could be evoked by a series of more than 150 stimuli applied in at least 8 cycles where the interval between two consecqutive pulses was alternatively ~20 s and smaller than 1 s. Take also note that at 0 mV the extrapolated time constant for deactivation ranged between 100 and 220 ms (see also Fig. 3 *C*) and therefore for signals in Fig. 6 *B* at most only 3% of channels were still open when the new hyperpolarizing (slow activating) stimulus was applied.

Corresponding experiments were performed on the single channel level as exemplified in Fig. 7. Single channel recordings observed in the fast mode with a time interval of 300 ms between consecutive pulses are displayed in the upper

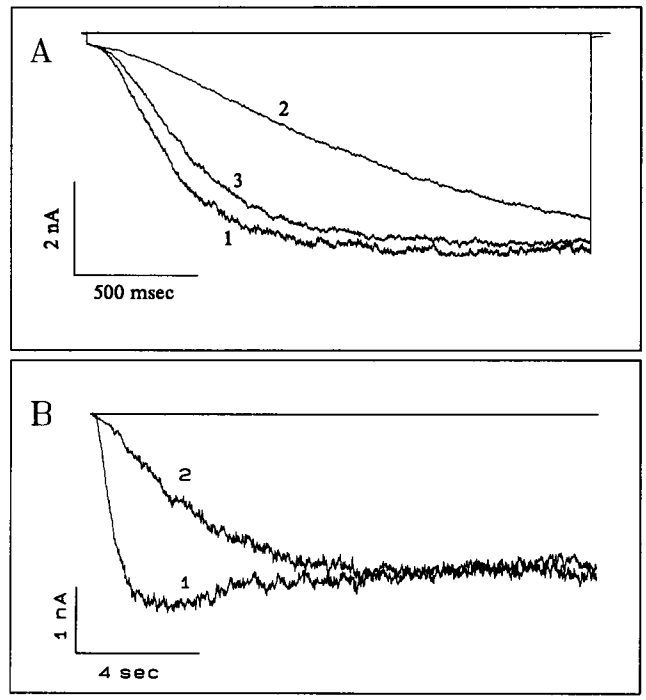

FIGURE 5 Fast and slow activation of vacuolar channels. Current responses induced by hyperpolarization to −100 mV compared for different voltage protocols. Precisely, curve 1 and 3 were obtained by applying to the vacuole a series of test pulses with a time interval of 20 s between the end of the test pulse and the beginning of the following one. When the interval between two consecutive pulses was reduced to 300 ms, current activation was much slower (*curve 2*). There is not much difference in the steady state current level reached by the two protocols (compare steady state in *B*). This effect is reversible. Curve 1 corresponds to the average obtained from five pulses before the stimulation at higher frequencies (average of 27 traces) and curve 3 represents the recovery averaged over nine traces. (*B*) Similar curves to those reported in *A* but on a longer time scale.

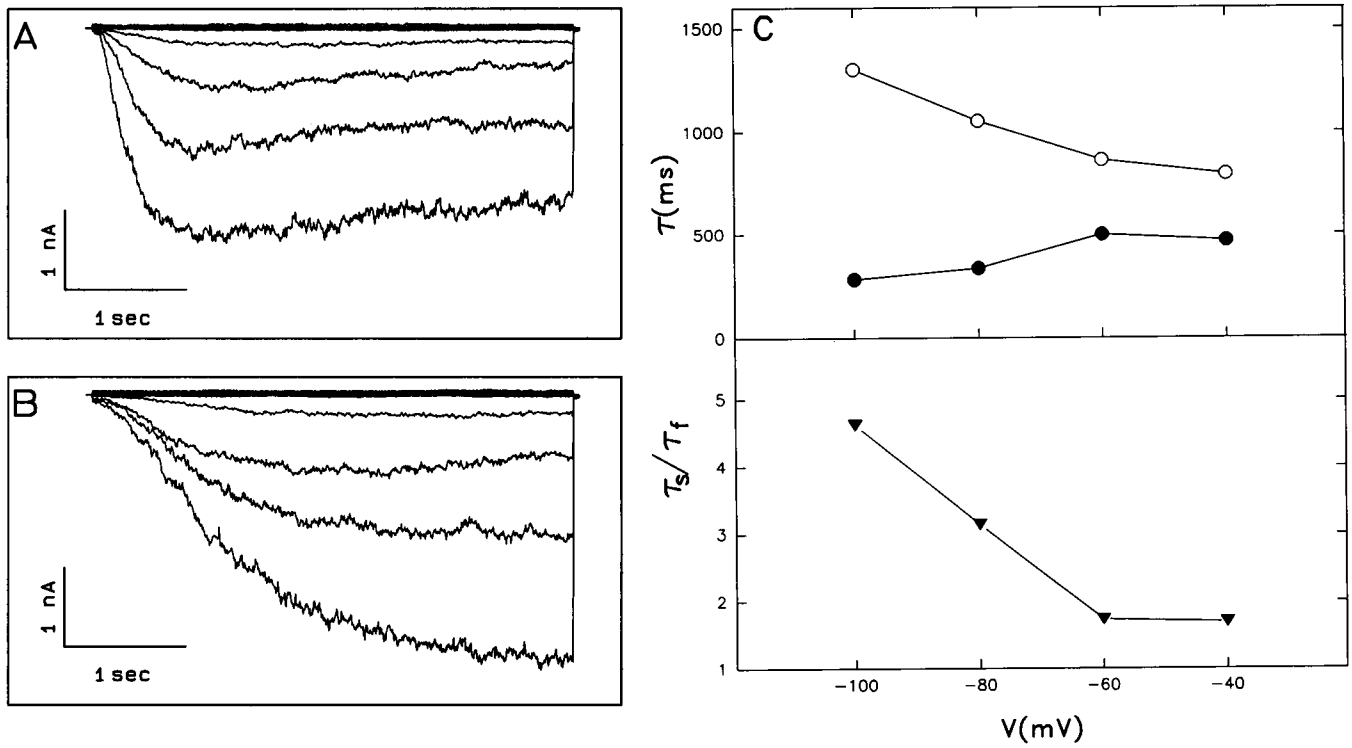

FIGURE 6 Current-voltage relation of fast and slow activation. Complete IV characteristics of the radish root vacuole current measured under whole cell patch clamp conditions using the low and high frequency stimulation protocol in *A* and *B*, respectively. Curves in *A* show a biphasic trend with a moderate (~15%) decline of the current which is not present in *B*. In *C*: Upper part: Time of activation, τ, versus the voltage of the stimulus for the fast (●) and slow (○) mode. Time interval: 16 s in fast mode, 740 ms in slow mode. Lower part: The ratio τ_s/τ_f between the slow and fast activation time constants is plotted versus the voltage of the stimulus.

half of the figure. Under these conditions, channels activated with time constants comparable to those of the whole-vacuole currents. Moreover, they showed a single channel conductance of ~90 pS and displayed no detectable inactivation during the voltage pulse. Similar results were obtained for single channels recorded in the slow mode which are displayed in the lower half of Fig. 7. The bottom trace was chosen to illustrate the occasional occurrence of a small single channel conductance which was already observed under steady state conditions. As these small conductances did not contribute significantly to the whole-vacuole current they were discarded in the present analysis. To summarize these results, the single channel recordings in the fast and slow mode were essentially indistinguishable from those observed under steady state recording conditions

DISCUSSION

Fast and slow activating currents are probably mediated by the same channel

Several lines of evidence suggest that the fast and slow activating currents are probably mediated by one channel type. First, only one mayor single channel conductance level was obtained in vacuole-attached membrane patches. Second, the pharmacological profile of vacuolar ion channels were quite uniform in the sense that fast and slow channels were blocked by vacuolar channel blockers (e.g., Zn^{2+}, see Fig. 4 *B* and Ni^{2+} (Gambale and Carpaneto, unpublished results)) and were both modulated by the cytosolic calcium concentration (Fig. 4 *A*). Third, the maximum current amplitude for fast and slow activating channels was comparable, rendering it very unlikely that a second population of channels was activated upon switching from slow to fast activation kinetics.

These considerations are also supported by data shown in Fig. 7 that presents single channels recorded in the fast and slow mode, respectively. Theoretically, the slow activation kinetics at high stimulation frequency might be explained by a second type of channel that displays a fast inactivation and therefore fails to open at higher stimulus frequency. However, this possibility is rendered unlikely by the fact that we did not find a fast inactivating channel in any of our single channel recordings. Moreover, the striking similarity between single channel currents obtained in the fast and slow mode strongly suggests that they were indeed carried by an identical channel population.

It is interesting to note that the properties of the vacuolar channels from radish roots were similar to the properties of vacuolar channels previously described in other systems. For example, voltage-dependent channels described in sugar beet vacuoles (Hedrich and Neher, 1987; Pantoja et al., 1992a, 1992b) displayed a voltage dependence, single channel conductance (~80 pS), calcium sensitivity, and block by Zn^{2+} similar to the channels observed in this report. Importantly, these observations suggest that the fast and slow activation

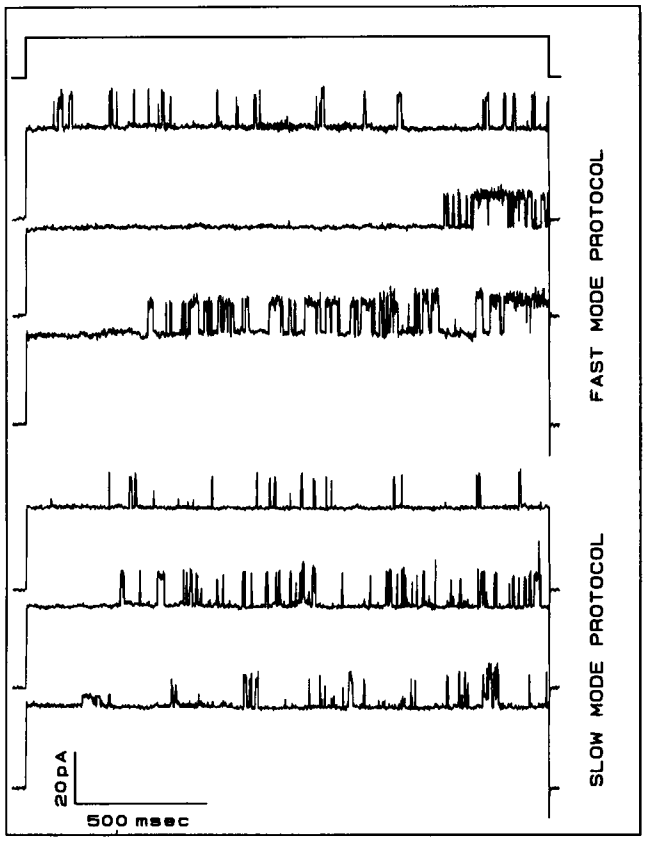

FIGURE 7 Comparison of single channels obtained by stimulating the vacuole with the two voltage protocols. Data were recorded in the vacuole-attached configuration. The upper trace represents a voltage step to +80 mV from a holding potential of 0 mV. Under the protocol eliciting the fast mode (i.e., the interval between two consecutive pulses ~300 ms) typical single channel events (in three upper traces) showed the same amplitude either if they appeared at the very beginning of the step voltage or at the end of the stimulus. No relevant differences were observed by systematically comparing signals as those represented in the upper traces with records obtained under the protocol eliciting the slow mode (i.e., interval between pulses > 10 s) as those shown in the three lower records. In single channel recordings we did not observe any inactivating channel.

modes of radish root channels might exist in plant vacuoles obtained from other tissue.

Different models can explain the fast and slow activation kinetics of ion channels in radish root vacuoles. For example, a formal description of the gating process is given by a voltage-dependent interconversion between two parallel modes of activation displayed in Scheme 1. Interestingly, this scheme has been proposed in earlier reports (Hess et al., 1984; Fenwick et al., 1982; Pietrobon and Hess, 1990; Ikeda et al., 1991; Bean, 1990) to explain the "facilitation" of voltage-dependent calcium currents in cardiac cells. In this system, depolarizing prepulses potentiated amplitudes of L-type calcium currents measured in the "whole cell" patch clamp configuration. On the single channel level, this augmentation was paralleled by long-lasting calcium channel openings, supporting a kinetic model with a forced conversion of the calcium channel to a new mode of activity. Spontaneous switching between the two modes was rarely observed, while chemical agonists evoked effects comparable to those induced by strong depolarizing voltages (Hess et al., 1984; Pietrobon and Hess, 1990). Clearly, these observations are not directly comparable to voltage-dependent ion channels in vacuoles, where voltage stimulation at high frequency induced a slower activation of currents. The basic kinetic formalism, however, might be adapted to vacuolar channels by assuming that fast and slow activation corresponds to a switch between two configurations characterized by different kinetic properties. This model can be schematized as follows (Hess et al., 1984):

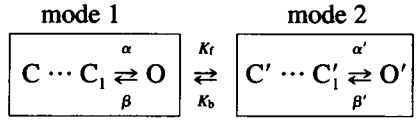

(1)

SCHEME 1

where K_f and K_b are the voltage-dependent forward and backward reaction rates connecting the two modes. The rate constants for the transitions between closed and open states will have different values depending on the mode (α, β for mode 1, and α', β' for mode 2). As it has been suggested for calcium channels, the rate constants for conversion between the two gating modes are supposed to be slow compared to "normal" channel opening and closing rates.

Another, and apparently simpler, mechanism is given by the following kinetic scheme:

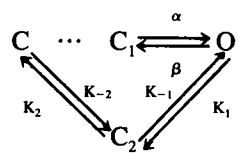

SCHEME 2

To illustrate the features of this model, the rate constants are assumed to be voltage-dependent so that, at hyperpolarizing voltages ($\alpha \gg \beta \sim K_1 \sim 0$), the channel from the closed state C will reach the open state O (possibly via other closed states (C_n)), but it will not proceed further to state C_2 unless the vacuole is depolarized. K_1 is assumed to be strongly voltage-dependent so that, at depolarizing voltages (if $K_1 \gg \beta$) the channel proceeds to the closed state C mainly via the state C_2. If, after the depolarization, a new stimulus is applied before the channel reaches state C, a slower kinetics (regulated mainly by rate K_2) can be observed. It is immediately evident that a voltage protocol (alternatively hyperpolarizing and depolarizing) could force the channel to proceed clockwise in Scheme 2 and that, depending on rate K_2, the interval between two stimuli δT, plays a central role on the activation kinetics.

To illustrate that this model may give rise to the desired properties, a preliminary computer simulation of the current time course was performed. As indicated in Fig. 8, the ionic current was derived by the analytical solution of the differential equations describing Scheme 2 under the assumptions denoted in the figure legend. The results for different time

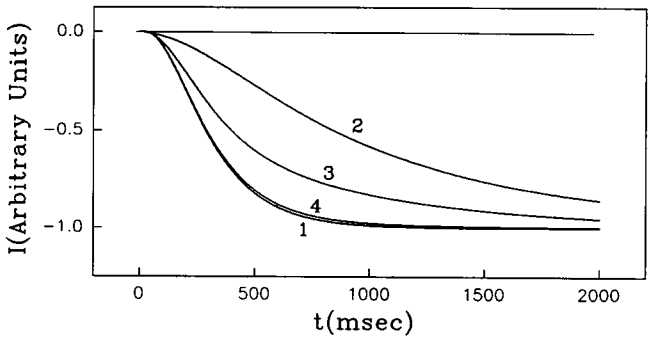

FIGURE 8 Simulation of fast and slow activation kinetics. Fast and slow activation kinetics were simulated by varying the time interval between two consecutive stimuli. δT = 0.5, 5, and 18 s for curves 2, 3, and 4 with respect to curve 1 (δT = 1). Values for the rate constants were partly derived from experimental data and in part imposed according to the mechanism described in the text. In particular, rates at −100 mV were assumed to be: K_2 = 1.25 s^{-1}, α = 5.5 s^{-1}, and $\beta \sim K_{-2} \sim K_{-1} \sim K_1 \sim 0$. Instead, when V = 0 mV it will be K_2 = 0.2 s^{-1}, K_1 = 6.66 s^{-1}, β = 0.1 s^{-1}, and $\alpha \sim K_{-2} \sim K_{-1} \sim 0$. It is immediate to see that at both voltages the principle of microscopic reversibility is satisfied if $K_1 = \beta K_{-2} K_{-1}/\alpha K_2$, in accordance with our hypothesis that K_1 is large when α is small and vice versa.

intervals between two consecutive stimuli are reported in Fig. 8. Note that curve 4 (δT = 18 s) shows almost 100% of recovery with respect to the current of the first stimulus (Curve 1). Basically, all rate constants were assumed to be voltage-dependent, although this does not exclude the possibility that also chemical activators participate in the modulation of current activation properties. In future investigations, a more detailed analysis is needed to identify the specific molecular processes that control the opening and closing of vacuolar ion channels. Eventually, the schemes described in this report might serve to elucidate the specific molecular processes which are involved in the voltage-dependent gating of ion channels in both plant and animal cells.

We greatly appreciated the contribution of Dr. Monica Bregante who collaborated in the single channel analysis.

Research supported by the Deutsche Forschungsgemeinschaft (DFG) and National Research Council of Italy, Special Project RAISA, subproject N:2, Paper N.1087).

REFERENCES

Bean, B. 1990. Gating for the physiologist. *Nature (Lond.)*. 348:192–193.

Fenwick, E. M., A. Marty, and E. Neher. 1982. Sodium and calcium channels in bovine chromaffin cells. *J. Physiol. (Lond.)*. 331:599–635.

Hamill, O. P., A. Marty, E. Neher, B. Sakmann, and F. Sigworth. 1981. Improved patch clamp techniques for high resolution current recording from cells and cell-free membrane patches. *Pflügers Arch.* 391:85–100.

Hedrich, R., and E. Neher. 1987. Cytoplasmic calcium regulates voltage dependent ion channels in plant vacuoles. *Nature (Lond.)*. 329:833–836.

Hedrich, R., and J. I. Schroeder. 1989. The physiology of ion channels and electrogenic pumps in higher plants. *Annu. Rev. Plant Phys.* 40:539–569.

Hess, P., J. B. Lansmann, and R. Tsien. 1984. Different modes of Ca-channel gating behaviour favoured by dihydropyridine Ca agonists and antagonists. *Nature (Lond.)*. 311:538–544.

Hille, B. 1992. Ionic channels of excitable membranes. Sinauer Publishing Co, New York.

Ikeda, S. R. 1991. Double pulse calcium channel current facilitation in adult rat sympathetic neurones. *J. Physiol. (Lond.)*. 439:181–214.

Keller, B. U., R. Hedrich, and K. Raschke. 1989. Voltage dependent anion channels in the plasma membrane of guard cells. *Nature (Lond.)*. 341: 450–453.

Pantoja, O., J. Dainty, and E. Blumwald. 1992a. Cytoplasmic chloride regulates cation channels in the vacuolar membrane of plant cells. *J. Membr. Biol.* 125:219–229.

Pantoja, O., A. Gelli, and E. Blumwald. 1992b. Voltage dependent calcium channels in plant vacuoles. *Science (Wash. DC)*. 255:1567–1569.

Pietrobon, D., and P. Hess. 1990. Novel mechanism of voltage dependent gating in L-type calcium channels. *Nature (Lond.)*. 346:651–655.

Schroeder, J. I., K. Raschke, and E. Neher. 1987. Voltage dependence of K^+-channels in guard cell protoplasts. *Proc. Natl. Acad. Sci. USA*. 84: 4108–4112.